Uptake of NO_3 on Water Solutions: Rate Coefficients for Reactions of NO_3 with Cloud Water Constituents

T. Imamura,[†] Y. Rudich,[‡] R. K. Talukdar,[§] R. W. Fox,[⊥] and A. R. Ravishankara*[,§,∥]

Aeronomy Laboratory, National Oceanic and Atmospheric Administration, Boulder, Colorado 80303

Received: September 13, 1996; In Final Form: January 6, 1997[⊗]

The reactive uptake coefficients, γ, of NO_3 onto aqueous solutions containing ions $X^- = HSO_3^-$, SO_3^{2-}, $HCOO^-$, CH_3COO^-, and OH^- were measured at 273 ± 1 K using a wetted-wall flow tube reactor. The values of $H^2D_l k$ (H = Henry's law coefficient, D_l = diffusion coefficient in the liquid phase, and k = second-order rate coefficient for the liquid phase reactions of NO_3 with X^-) for the reactive uptake of NO_3 were determined by measuring γ as a function of liquid phase reactant concentration. The linear correlation between the measured rate coefficients and those for corresponding SO_4^- reactions, and the dependence of the measured rate coefficients on the redox potential of the X/X^- pair suggest that the $NO_3 + X^-$ reactions proceed by electron transfer. The atmospheric implications of these findings are briefly discussed.

Introduction

The nitrate radical, NO_3, formed primarily by the reaction of NO_2 with O_3 in the gas phase, is an important nighttime gas phase oxidant in the atmosphere.[1,2] The NO_3 radical can also be an important nighttime oxidant in atmospheric droplets and aerosol,[3−6] which contain dissolved species such as SO_2, HSO_3^-, SO_3^{2-}, organic acids (such as formic acid, acetic acid), and halides (in the marine boundary layer).[7−9] The liquid phase reactions of NO_3 with these species can initiate the catalytic oxidation of S(IV) via the formation of radical species such as OH, SO_3^-, and Cl_2^-.[3,4,6] The uptake of NO_3 into cloud droplets and aerosol is governed by its solubility, liquid phase diffusion, and reactions in the liquid phase. Therefore the rate coefficients for the reactions of NO_3 with the constituents mentioned above, under atmospheric pH and salt concentrations, are needed to assess the role of the heterogeneous reactions of NO_3 in the troposphere.

Second-order rate coefficients for the reactions of NO_3 with several ions have been measured in the bulk liquid phase.[10−14] However, the agreement between the rate coefficients measured in pulsed radiolysis[11,12] and laser photolysis studies[13] is poor for some reactions. For example, the rate coefficient for the reaction of NO_3 with Cl^- measured using laser photolysis[13] is about an order of magnitude smaller than those obtained by pulsed radiolysis studies.[11,12] This disagreement was attributed to the ionic strength effect on the neutral−ion reaction.[13]

Recently, we initiated studies on heterogeneous chemistry of NO_3. In previous papers,[15,16] we reported the reactive uptake coefficients of NO_3 on water and some ionic solutions and proposed that NO_3 was taken up irreversibly by liquid water due to reaction 1:

$$NO_3(aq) + H_2O(l) \xrightarrow{k_1} \text{products} \quad (1)$$

NO_3 uptake was found to be controlled by reactive losses in the liquid phase. Furthermore, the rate coefficients for the reactions of NO_3 with halide ions in solution increase with decrease in redox potentials.

In this paper, we report the relative rate coefficients for the liquid phase reactions of NO_3, reactions 2−6, obtained by measuring uptake coefficients of NO_3 into aqueous solutions using a wetted-wall flow tube reactor:

$$NO_3(aq) + HSO_3^- \xrightarrow{k_2} \text{products} \quad (2)$$

$$NO_3(aq) + SO_3^{2-} \xrightarrow{k_3} \text{products} \quad (3)$$

$$NO_3(aq) + OH^- \xrightarrow{k_4} \text{products} \quad (4)$$

$$NO_3(aq) + HCOO^- \xrightarrow{k_5} \text{products} \quad (5)$$

$$NO_3(aq) + CH_3COO^- \xrightarrow{k_6} \text{products} \quad (6)$$

A possible mechanism for the liquid phase reactions of NO_3 and the atmospheric implications of these results are also discussed.

Experimental Section

A wetted-wall flow tube reactor was combined with NO_3 detection through a long-path 662 nm absorption to measure its uptake coefficients onto aqueous solutions. The details of the experimental setup were described previously.[15,16] Briefly, NO_3 was generated by thermal dissociation of N_2O_5 in an oven maintained at 400 K and was introduced into a flow reactor (i.d. = 1.9 cm) through a movable injector (i.d. = 0.53 cm). NO_3 was detected by measuring its absorbance at 662 nm (from a tunable diode laser) in a long-path White-type absorption cell (optical path length = 1260 cm). The initial concentration of NO_3 used in this work was in the range of $(2-20) \times 10^{11}$ cm^{-3}.

The flow rates of the liquid film were in the range 1.3−4 cm^3 s^{-1}. The thickness and the flow velocity of the liquid film

[†] NOAA/National Research Council Senior Research Associate (Permanent address: National Institute for Environmental Studies, Tsukuba, Ibaraki 305, Japan).

[‡] NOAA/National Research Council Post-Doctoral Research Associate. Current address: Department of Environmental Sciences, Weizmann Institute of Science, Rehovot 76100, Israel.

[§] Also affiliated with the Cooperative Institute for Research in Environmental Sciences, University of Colorado, Boulder, CO 80309.

[⊥] National Institute of Standards and Technology, Time and Frequency Division, Boulder, CO 80303.

[∥] Also associated with the Department of Chemistry and Biochemistry, University of Colorado, Boulder, CO 80303.

[⊗] Abstract published in *Advance ACS Abstracts,* February 15, 1997.

S1089-5639(96)02787-9 CCC: $14.00

were calculated to be ~0.025 cm and ~10 cm s^{-1}, respectively. To minimize evaporation of water from the liquid film, water vapor from a saturator was added to the main He flow. The flow velocity of the carrier gas was varied between 500 and 1600 cm s^{-1}. All experiments were performed at 273 ± 1 K and at a total pressure of 10−16 Torr.

Reagent grade chemicals, NaCl, NaOH, $NaHSO_3$, Na_2SO_3, HCOONa, CH_3COOK, and $NaNO_3$, were used without further purification. The solutions were prepared using deaerated deionized water (>17.5 MΩ cm). The concentrations of formate and acetate ions from the weak acids, formic and acetic acids, were calculated using the pH of the solution, the salt concentrations, and the dissociation constants K_a. The pH of the solution measured by a pH meter was adjusted by adding NaOH. In the case of HSO_3^- and SO_3^{2-}, the total concentration of S(IV) ([S(IV)] ≡ [SO_2(aq)] + [HSO_3^-(aq)] + [SO_3^{2-}(aq)]) was determined before and after each uptake measurement by iodometric titration.[17] The concentration of each species was calculated using the first and second dissociation constants of H_2SO_3. The OH^- concentration was determined before and after each experiment by titration with standard sulfuric acid solution. The concentrations of anions of strong acids were taken to be the salt concentration in the solution.

Results

First-order loss rate coefficients of NO_3 due to uptake on aqueous solutions were measured by monitoring its concentration in the gas phase as a function of relative injector positions. A plot of ln [NO_3] vs relative injector position was a line with a slope (cm^{-1}) of $-k_o$, from which the first-order rate coefficient, $k_m = k_o v_g$ (s^{-1}), was calculated. Here, v_g is the gas flow velocity in the flow tube (cm s^{-1}). The measured value of k_m was corrected for the radial concentration gradient generated due to the uptake of NO_3 at the wall and to gas phase diffusion limitation to obtain k_c, the corrected first order rate coefficient, using the method developed by Brown.[18] The diffusion coefficient of NO_3 in He was taken to be 370 and 100 Torr cm^2 s^{-1} in H_2O vapor at 273 K.[15,16]

The uptake coefficient γ was calculated from k_c:[19]

$$\gamma = (2r/\omega)k_c \qquad \text{(I)}$$

where ω is the average molecular speed of NO_3 (cm s^{-1}) and r is the effective flow-tube radius (0.925 cm). γ is related to the reactive loss in the liquid:[20−23]

$$\frac{1}{\gamma} = \frac{1}{\alpha} + \frac{\omega}{4RTH\sqrt{D_l k_l'}} \qquad \text{(II)}$$

where α is the mass accommodation coefficient of NO_3 in water, R is the gas constant (0.082 L atm mol^{-1} K^{-1}), T is the temperature (K), H is the Henry's law constant (M atm^{-1}), D_l is the diffusion coefficient of NO_3 in the solution (cm^2 s^{-1}), and k_l' is the first-order rate coefficient for NO_3 reaction in the solution (s^{-1}). Since the uptake of NO_3 onto the aqueous solution is limited by reactive loss in the solution, that is $\alpha >> \gamma$, as previously reported,[15] eq II is reduced to

$$\gamma^2 = (4RT/\omega)^2 H^2 D_l k_l' \qquad \text{(III)}$$

In the aqueous phase, k_l' is given by[15]

$$k_l' = k_1' + k_i a_x \qquad \text{(IV)}$$

where k_1' is the first-order loss rate coefficient due to the reaction with water (reaction 1), k_i is the second-order rate coefficient for the reaction with X^- ions (reaction i), and a_x is the activity of X^- ion. The activity is defined as the product of the concentration and the activity coefficients. The activity coefficients were taken from the literature where available.[24,25] In the case of $NaHSO_3$ and Na_2SO_3, they were calculated using Debye−Huckel theory for dilute solutions. In pure water (reaction 1), the uptake coefficient γ_w determined[15] to be (2.0 ± 0.5) × 10^{-4} is given by

$$\gamma_w^2 = (4RT/\omega)^2 H^2 D_l k_l' \qquad \text{(V)}$$

Combining eqs III−V, we obtain

$$\gamma^2 - \gamma_w^2 = (4RT/\omega)^2 H^2 D_l k_i a_x \qquad \text{(VIa)}$$

Equation VIa can be rewritten as

$$\log(\gamma^2 - \gamma_w^2) = \log\{(4RT/\omega)^2 H^2 D_l k_i\} + \log(a_x) \qquad \text{(VIb)}$$

If the uptake is limited by reactive loss in the bulk liquid phase, plots of $\log(\gamma^2 - \gamma_w^2)$ vs $\log(a_x)$ are expected to yield straight lines with slope equal to unity; $H^2 D_l k_i$ is obtained from the intercept, i.e., when $a_x = 1$. As an example, plots of $\log(\gamma^2 - \gamma_w^2)$ vs $\log(a_x)$ for $X^- = SO_3^{2-}$, OH^- and $HCOO^-$ are shown in Figure 1. The slopes of these plots were determined to be 0.9 ± 0.2, 1.0 ± 0.2, and 1.0 ± 0.2 for the reactions with SO_3^{2-}, OH^-, and $HCOO^-$ ions, respectively. The quoted errors are 2σ (precision from unweighted fit to eq VIb). As expected, the slopes for reactants investigated here are ~1, validating the assumption that the uptake of NO_3 onto an ionic solution is due to reactions in the bulk liquid phase and not on the surface of the flowing liquid. The values of $H^2 D_l k_i$ for reactions 2−6 measured here are listed in Table 1 along with those for reactions 7−10 reported previously:[15,16]

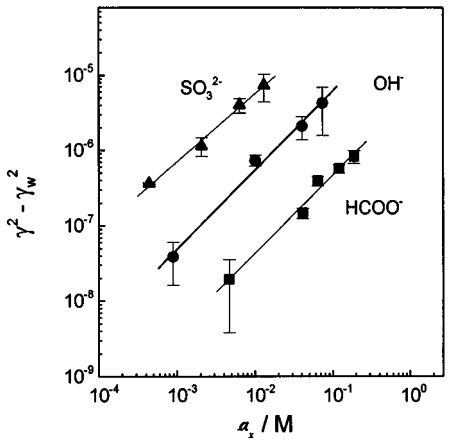

Figure 1. Plots of $\log(\gamma^2 - \gamma_w^2)$ as a function of $\log(a_x)$ for X = SO_3^{2-} (solid triangles), OH^- (solid circles), and $HCOO^-$ (solid squares). The error bars are 2σ precision only.

$$NO_3(aq) + Cl^- \xrightarrow{k_7} \text{products} \qquad (7)$$

$$NO_3(aq) + Br^- \xrightarrow{k_8} \text{products} \qquad (8)$$

$$NO_3(aq) + I^- \xrightarrow{k_9} \text{products} \qquad (9)$$

$$NO_3(aq) + NO_2^- \xrightarrow{k_{10}} \text{products} \qquad (10)$$

The quoted errors are 2σ and include both precision and estimated systematic errors, which are discussed below. The

TABLE 1: Rate Coefficients for Reactions of NO_3 with Several Ions

reaction (ion)	$H^2D_l\ k_\gamma$,[a] M cm^2 atm^{-2} s^{-2}	$k_\gamma/k_{7\gamma}$	k_γ,[b] M^{-1} s^{-1}	k_b,[c] M^{-1} s^{-1} (273 K)
R2 (HSO_3^-)	$1.0^{+0.3}_{-0.2} \times 10^2$	$1.0^{+0.5}_{-0.4} \times 10^1$	2.9×10^7	7.2×10^8 LP, Exner *et al.* (1992)
R3 (SO_3^{2-})	$6.5^{+2.7}_{-1.9} \times 10^1$	$6.5^{+3.7}_{-2.7}$	1.8×10^7	2.6×10^8 LP, Exner *et al.* (1992)
R4 (OH^-)	$7.7^{+3.0}_{-2.7}$	$7.7^{+4.3}_{-3.6} \times 10^{-1}$	2.1×10^6	4.1×10^7 LP, Exner *et al.* (1992)
R5 ($HCOO^-$)	$5.1^{+2.0}_{-1.5} \times 10^{-1}$	$5.1^{+2.9}_{-2.1} \times 10^{-2}$	1.4×10^5	2.6×10^7 LP, Exner *et al.* (1994)
R6 (CH_3COO^-)	$3.8^{+1.5}_{-1.3} \times 10^{-1}$	$3.8^{+2.1}_{-1.7} \times 10^{-2}$	1.1×10^5	9.1×10^5 LP, Exner *et al.* (1994)
R7 (Cl^-)	$1.0^{+0.4}_{-0.3} \times 10^1$	(reference)	2.8×10^6	2.8×10^6 LP, Exner *et al.* (1992)
				2.7×10^7 PR, Kim and Hamill (1976)
				2.2×10^7 PR, Neta and Huie (1986)
R8 (Br^-)	$3.6^{+1.7}_{-1.1} \times 10^2$	$3.6^{+2.2}_{-1.5} \times 10^1$	1.0×10^8	2.4×10^9 PR, Neta and Huie (1986)
R9 (I^-)	$1.7^{+0.7}_{-0.4} \times 10^4$	$1.7^{+1.0}_{-0.6} \times 10^3$	4.6×10^9	5.2×10^9 diffusion-controlled value
R10 (NO_2^-)	$6.7^{+2.7}_{-1.9} \times 10^2$	$6.7^{+3.8}_{-2.8} \times 10^1$	1.8×10^8	6.6×10^8 PR, Daniels (1969)

[a] Errors are 2σ which include precision and systematic errors. (See text.) [b] Values were calculated using $k_7 = 2.8 \times 10^6$ M^{-1} s^{-1} at 273 K as a reference.[13] (See text.) [c] Values at 273 K were calculated using the reported activation energies[13,14] for reactions 2 and 4−7 and 16 kJ mol^{-1} for reactions 3, 8, and 10. LP, laser photolysis; PR, pulsed radiolysis.

second-order rate coefficients for reactions 2−6 and 8−10 calculated by assuming $k_7 = 2.8 \times 10^6$ M^{-1} s^{-1} are also shown in Table 1. Therefore, we have implicitly assumed H^2D_l to be $(3.6 \pm 1.0) \times 10^{-6}$ M^2 atm^{-2} cm^2 s^{-1}, the value deduced in our previous work which also used $k_7 = 2.8 \times 10^6$ M^{-1} s^{-1}.[15]

Discussion

Possible Sources of Errors in γ. In the present work, uncertainties in the water vapor pressure in the flow reactor, the diffusion coefficient of NO_3 in the gas phase, and simultaneous occurrence of gas and liquid phase reactions of NO_3 are the major sources of error in the measured values of γ. A change of pH at the surface of the liquid film due to uptake of NO_3 and N_2O_5 could be an additional source of error.

Water vapor in the flow reactor influences both the gas phase diffusion coefficients of NO_3 and the gas flow velocity in the reactor. We introduced He saturated with water vapor into the flow reactor to minimize evaporation and cooling of the liquid film. The temperature of the liquid film was measured by thermocouples at different locations along the liquid flow and was found to be the same within 1 K. The uncertainty in the water vapor pressure due to the uncertainty in the water temperature ($\Delta T = \pm 1$ K) is estimated to be within ± 0.3 Torr. For measurements of $\gamma \leq 3 \times 10^{-3}$, the error associated with the uncertainty in the water vapor pressure is estimated to be $\leq^{+12\%}_{-9\%}$. The asymmetry in the uncertainty is due to the nonlinear dependence of γ on water vapor pressure.

The pressure-dependent diffusion coefficient of NO_3, D_c, used in this work is estimated to be accurate to $\pm 20\%$ as reported previously.[16] For low values of the uptake coefficient, i.e., $\gamma \leq 3 \times 10^{-3}$, an uncertainty in D_c of 20% translates to an uncertainty in γ of $\leq^{+30\%}_{-15\%}$. The estimated errors due to uncertainties in vapor pressure of water and D_c are conservative, and overall uncertainty in γ is estimated to be $\leq^{33\%}_{17\%}$.

NO_3 can also react with NO_2 in the reactor

$$NO_3 + NO_2 + M \rightleftarrows N_2O_5 + M \qquad (11)$$

N_2O_5 formed by reaction 11 could be lost on water at a (gas phase) diffusion-limited rate. Since the first-order rate coefficient k_g due to gas phase reactions is expected to be small as discussed below, the overall first-order rate coefficient for loss of NO_3, k_{mp}, measured in the presence of gas phase reactions would be given by

$$k_{mp} = k_{ma} + k_g \qquad (VII)$$

where k_{ma} is the first-order rate coefficient of NO_3 loss measured in the absence of gas phase reactions and due only to uptake at the walls. In such a case, k_c used to obtain γ should be calculated using k_{ma} instead of k_{mp}. Otherwise, the gas phase loss would be included with the heterogeneous loss and lead to an overestimation of γ. Strictly, k_c is obtained numerically following the procedure discussed by Brown.[18] As the value of k_g increases, the error introduced using expression VII would increase; for example, for $k_{mp} = 20$ s^{-1}, errors are ~1%, ~5%, and ~10% for $k_g = 1$, 5, and 10 s^{-1}, respectively. A complete analysis, which includes corrections due to radial and axial concentration gradients as a result of the uptake at the wall and gas phase loss, needs to be performed when the contribution of k_g to the measured k_{mp} is large. Under our experimental conditions ($T = 273$ K, $P_{total} = 10-17$ Torr), the second-order rate coefficient for reaction 11 was measured to be 3×10^{-13} cm^3 molecule^{-1} s^{-1}.[15] The concentration of NO_2 in the reactor is expected to be $\sim[NO_3]_0$, which is in the range of $(2-20) \times 10^{11}$ molecule cm^{-3}. Thus, the first-order rate coefficient of NO_3 loss due to reaction 11 must be <1 s^{-1}. Therefore the error due to gas phase loss of NO_3 is estimated to be $\leq 30\%$ for $\gamma = 2 \times 10^{-4}$ and $\leq 5\%$ for $\gamma = 3 \times 10^{-3}$. The measured values of γ were independent of the initial NO_3 concentration; hence, the error in γ from the gas phase reaction is smaller than the precision in the measured γ values.

Another possible source of error is a pH change at the surface of the liquid due to the uptake of N_2O_5 formed by reaction 11 and the effect of this variation on measured values of γ. The concentration of a conjugate base (A^-) of a weak acid (AH) is controlled by the pH of the aqueous solution via the equilibrium reaction

$$A^-(aq) + H_2O(l) \rightleftarrows AH(aq) + OH^-(aq) \qquad (12)$$

The ratio of activities of A^- and AH is obtained using the dissociation constant K_a of AH

$$a(A^-)/a(AH) = K_a/a(H^+) \qquad (VIII)$$

where a is the activity. The effective thickness of the liquid

surface for NO_3 uptake, l, is expressed by the diffuso-reactive length, $l = \sqrt{D_l/k_l'}$, and is much thinner than the thickness δ of the liquid film; e.g., $l = 10^{-5}$ cm for $D_l = 10^{-5}$ cm^2 s^{-1} and $k_l' = 10^5$ s^{-1} while $\delta = 0.025$ cm. Hence, the pH at the liquid surface must be known to estimate the effective concentration of A^-. In this work, the pH at the liquid surface is likely to change due to the uptake of N_2O_5 to form HNO_3. To assess this contribution, the concentration of the NO_3^- ion in the water (3.5 L total volume) circulating through the reactor was measured by ion chromatography.[15] After the circulating water was exposed to NO_3 for 3 h, the NO_3^- concentration in the solution was measured to be 3.2×10^{-5} M. The average formation rate of NO_3^- (and H^+) in the liquid is, then, calculated to be $\sim 1 \times 10^{-8}$ mol s^{-1}. Under a plug flow approximation, the average H^+ concentration $[H^+]_s^{av}$ at the liquid surface due to the uptake of N_2O_5 is estimated to increase by $\leq 3 \times 10^{-5}$ M. Estimation of the surface concentration is described in the Appendix. This increase is less than 10% of the concentrations of OH^- and SO_3^{2-} in the solution and less than 1% of $HCOO^-$ and CH_3COO^- concentrations. Therefore, we conclude that such a pH change at the surface is negligible and does not change the ion concentration at the surface.

Comparison with Previous Studies. To place our measured relative rate coefficients for the $NO_3 + X^-$ reactions on an absolute scale, we need at least one absolute rate coefficient. As reported in our previous publication,[15] the absolute values of the rate coefficients, k_2 through k_{10}, were obtained from the measured $H^2D_l k$ and an extrapolation of Exner *et al.*'s value of $k_7 = 2.8 \times 10^6$ M^{-1} s^{-1} at 273 K.[13] This rate coefficient leads to $H^2D_l = (3.6 \pm 1.0) \times 10^{-6}$ M^2 atm^{-2} cm^2 s^{-1}. The measured relative values and those normalized to k_7, given by Exner *et al.*, are listed in Table 1. For comparison, the rate coefficients measured in the bulk phase are also listed. Hereafter, the subscripts γ and b are used to distinguish between rate coefficients obtained from our uptake measurements and bulk phase data found in the literature.

Figure 2 shows a plot of $\log(k_\gamma)$ vs $\log(k_b)$ for reactions 2−10. The k_b values, when not available at 273 K, were calculated using the reported activation energies[13,14] except for reactions 3 and 8−10. For reactions 3, 8, and 10, the activation energies have not been reported. However, our data show that the rate coefficients for these reactions are comparable to or larger than k_2. The activation energy for reaction 2 was reported to be 16 kJ mol^{-1},[13] which is nearly the value of 20 kJ mol^{-1} for the variation of the viscosity of water with temperature. Therefore, the activation energy (16 kJ mol^{-1}) for reaction 2 was used as those for reactions 3, 8, and 10. To our knowledge, k_b value for the reaction of NO_3 with I^- (reaction 9) is not measured. However, our data shows that this reaction is very fast. Therefore, we used diffusion-controlled rate coefficient, given by the expression[26]

$$k_9 = 4\pi R^* D N_A \qquad \text{(IX)}$$

where R^* is some critical distance, D is the diffusion coefficient in the liquid phase, and N_A is Avogadro's number. R^* was assumed to be the sum of radii of I^- (2.2×10^{-8} cm)[26] and NO_3 (1.2×10^{-8} cm).[15] D at 273 K was assumed to be the sum of the diffusion coefficients of I^- (1×10^{-5} cm^2 s^{-1})[26] and NO_3 (1×10^{-5} cm^2 s^{-1})[15] in water.

In Figure 2, the solid line corresponds to $k_\gamma = k_b$. It is found that the k_γ values are smaller than the k_b values for most of the reactions studied here and that the value of $k_{9\gamma}$ is essentially diffusion-controlled. On the other hand, there is a linear correlation (dotted line in Figure 2) between $\log(k_\gamma)$ and $\log(k_b)$ when the reactions of NO_3 with $HCOO^-$ (reaction 5), Cl^- (reaction 7, photolysis study), and I^- (reaction 9) ions are ignored. (Note: here we are comparing the measured rate coefficient for I^- with that calculated.) The slope of the line is 0.92 ± 0.23 (errors are 2σ and precision from unweighted fit only). Since the plot shown in Figure 2 is on log−log scale, the linear correlation does not depend on the rate coefficient of the reference reaction. The slope of ~ 1 indicates that $k_{i\gamma}$ is proportional to corresponding k_{ib}:

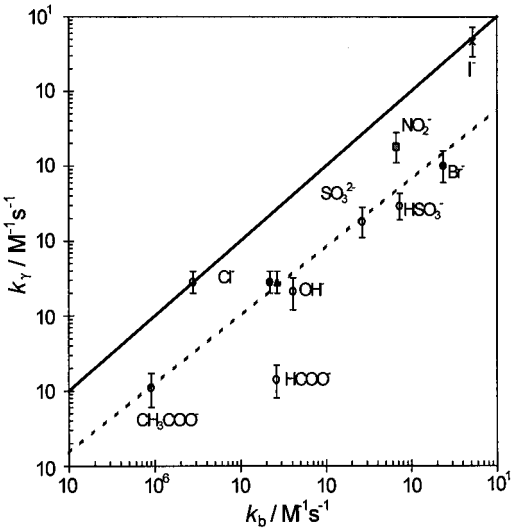

Figure 2. Plots of $\log(k_\gamma)$ as a function of $\log(k_b)$. k_γ's were calculated using $H^2D_l = (3.6 \pm 1.3) \times 10^{-6}$ M^2 atm^{-2} cm^2 s^{-1}. Values of k_b are from Daniels[10] (pulsed radiolysis, solid square), Kim and Hamill[11] (pulsed radiolysis, solid triangle), Neta and Huie[12] (pulsed radiolysis, solid circles), and Exner *et al.*[13,14] (laser photolysis study, open circles). Values of k_b at 273 K were extracted using the reported activation energies for the reactions with Cl^-, HSO_3^-, OH^-, $HCOO^-$, and CH_3COO^- ions[13,14] and 16 kJ mol^{-1} for the reactions with Br^-, NO_2^-, and SO_3^{2-} ions. For the reaction with I^-, diffusion-controlled rate coefficient was used as k_{9b}. The solid line corresponds to $k_\gamma = k_b$ and the dotted line shows a linear correlation between $\log(k_\gamma)$ and $\log(k_b)$ with the exception of reactions of NO_3 with $HCOO^-$, Cl^- (photolysis study), and I^-.

$$k_{i\gamma} = \text{constant} \times k_{ib} \qquad \text{(X)}$$

From the unweighted average of the ratios of $k_{ib}/k_{i\gamma}$, the proportionality constant was calculated to be 14 ± 8 where the error is 1σ and precision only. Therefore, it is possible that the $NO_3 + Cl^-$ reaction is not a good choice for a reference reaction and all our rate coefficients are ~ 15 times smaller. If the rate coefficients are 15 times larger, our measured γ yields $H^2D_l = 2.5 \times 10^{-7}$ M^2 atm^{-2} cm^2 s. However, such a low value for H^2D_l leads to other inconsistencies. For example, the value of $k_{9\gamma} = 6 \times 10^{10}$ M^{-1} s^{-1} is much larger than the estimated diffusion-controlled rate coefficient. Furthermore, the value of $k_{1\gamma}' = 1.8 \times 10^4$ s^{-1} is orders of magnitude larger than any reported first-order loss rate constant for loss of NO_3 in water.[13,14,27] Therefore, it is not clear why this discrepancy between k_γ and k_b exists. A reliable rate coefficient for a reference reaction is essential. The possibility that there is an intrinsic reason for not measuring k_b in our experimental approach cannot be discounted even though the measured values of γ depend on the square root of k_l', as is expected for a bulk phase reaction.

The larger disagreement between k_γ and k_b values for the reaction of NO_3 with $HCOO^-$ (reaction 5) compared to other reactions discussed above is not understood. k_{5b} was measured by Exner *et al.* using laser photolysis.[14] They also measured the rate coefficient for the reaction of NO_3 with undissociated

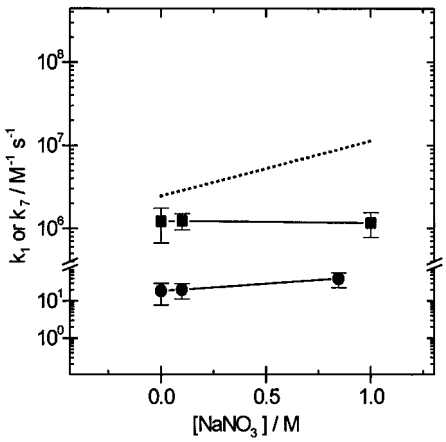

Figure 3. Plots of $k_{1\gamma}$ and $k_{7\gamma}$ as a function of [$NaNO_3$] for the reactions of NO_3 with water (reaction 1) and Cl^- (reaction 7). Solid circles: [NaCl] = 0 M. Solid squares: [NaCl] = 1.2×10^{-2} M. The error bars are 2σ precision only. The dotted line represents the effect of ionic strength on k_{7b} measured by Exner *et al.*[13] The values of k_{7b} at 273 K were extracted using the reported activation energy.[13]

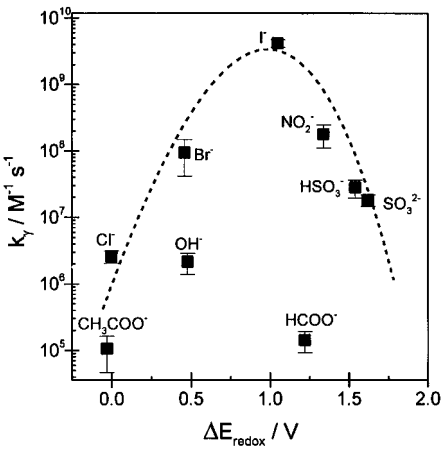

Figure 4. Plots of rate coefficients of NO_3 reactions, k_γ's, against the difference of redox potentials of X/X^- and NO_3/NO_3^- pairs. The broken line is merely a guide. Redox potentials of X/X^- are obtained from Rudich *et al.*[15] for $X^- = NO_3$ and from Stanbury[36] for $X^- = Cl^-$, Br^-, I^-, NO_2^-, SO_3^{2-}, OH^-, and $HCOO^-$ and from Exner *et al.*[14] for $X^- = HSO_3^-$ and CH_3COO^-.

HCOOH at pH = 0.5, which is extrapolated to be 1.3×10^5 M^{-1} s^{-1} at 273 K. Their rate coefficient for the reaction of NO_3 with HCOOH is close to the value of $k_{5\gamma}$ obtained in this work. However, the loss of NO_3 due to the reaction with HCOOH can be neglected in the pH range (pH = 6.8−8.2) maintained in our experiments. Furthermore, the pH change at the liquid surface was too small to form HCOOH. Hence, the reaction of NO_3 with HCOOH could not be important in our experiments.

The reason for the discrepancy between our relative rate coefficients and the absolute bulk phase liquid values is not clear. In our system, NO_3 was generated in the gas phase and was taken up by the reactions in the liquid phase just as in the atmospheric transfer of gas phase NO_3 to liquid droplets. In the absence of absolute rate coefficients in the liquid phase, our measured $H^2D_l k$ values can be used for atmospheric modeling.

Ionic Strength Effect (*I*) on γ. The rate coefficient for the reaction of NO_3 with Cl^-, k_{7b}, at room temperature was measured to be 7×10^7 and 1×10^8 M^{-1} s^{-1} using pulsed radiolysis at high ionic strength ($I \geq 2$ M)[11,12] and 1×10^7 M^{-1} s^{-1} using laser photolysis ($I = 0.11$ M).[13] Exner *et al.*[13] attributed the discrepancy between the results of the pulsed radiolysis and laser photolysis studies to the effect of ionic strength on the rate coefficient. They reported that the reaction rate coefficients changed with ionic strength from $k_{7b} = 1 \times 10^7$ at $I = 0.11$ to 4.2×10^7 M^{-1} s^{-1} at $I = 1$ M.

The ionic strength effect observed by Exner *et al.*[13] is large and should be detectable in our γ measurements. Therefore, the values of γ for reactions 1 and 7 were measured as a function of ionic strength by adding $NaNO_3$ to the solution. Since NO_3^- from $NaNO_3$ does not react with Na^+ or Cl^-, and the reaction of NO_3 with NO_3^- is merely a charge exchange, addition of $NaNO_3$ should not introduce any new loss processes for NO_3. Since the viscosities of water and 1 M $NaNO_3$ solution at 293 K ($\eta/\eta_w = 1.06$[28]) are essentially the same, the liquid phase diffusion coefficient of NO_3 at 273 K should also be constant. Using eqs III−V, the values of $H^2D_l k_{1\gamma}'$ and $H^2D_l k_{7\gamma}$ were obtained. Plots of $k_{1\gamma}$ and $k_{7\gamma}$, calculated using $H^2D_l = 3.6 \times 10^{-6}$ M^2 atm^{-2} cm^2 s^{-1}, against the concentration of $NaNO_3$ at two concentrations of added $NaNO_3$ are shown in Figure 3. Here we assume that the activity coefficient for Cl^- is not affected by the concentration of $NaNO_3$ (i.e., the ionic strength). Here, k_1 is defined as $k_1 = k_1'/(a_{H_2O}[H_2O])$. As can be seen in Figure 3, there is no visible effect of ionic strength on $k_{1\gamma}$ and $k_{7\gamma}$. The reason for the disagreement between our results and those of Exner *et al.*[13] is not understood.

Reaction Mechanism. The reactions of NO_3 with anions studied in this work are believed to be electron transfer processes.[13,14] The rate coefficient for outer-sphere electron transfer is known to depend on the difference in Gibbs free energy between the reactant and the product,[29] which is proportional to ΔE_{redox}, the difference in the redox potentials of X/X^- and NO_3/NO_3^- pairs. Figure 4 shows a plot of log-(k_γ) as a function of ΔE_{redox}. As can be seen in the figure, for $\Delta E_{redox} < 1$ V, the rate coefficients increase with increasing ΔE_{redox}. On the other hand, for $\Delta E_{redox} > 1$V, the rate coefficients decrease with increasing ΔE_{redox}. This overall feature (parabolic behavior) seen in Figure 4 is qualitatively consistent with Marcus theory for electron transfer reactions.[29]

The redox potential of SO_4^-/SO_4^{2-} pair is calculated to be 0.02 V lower than that of NO_3/NO_3^- pair from the measured rate coefficients for the forward and reverse reactions[13,30]

$$SO_4^- + NO_3^- \rightleftarrows SO_4^{2-} + NO_3 \qquad (13)$$

The $SO_4^- + X^-$ reactions are believed to be electron transfer processes.[31] Therefore, we expect a correlation between SO_4^- radical reactions and those of NO_3. The rate coefficients for the NO_3 reactions determined here are compared to those for corresponding SO_4^- reactions, $k_b(SO_4^-)$, in Figure 5. Because the rate coefficients for $SO_4^- + X^-$ reactions at 273 K are not available, the values at room temperature were used.[32,33] With the exception of $HCOO^-$ and I^- reactions, a linear correlation between NO_3 and SO_4^- reaction rate coefficients is observed. The slope of the line is 1.2 ± 0.4 (error is 2σ precision derived from unweighted fit). This slope of near unity suggests that NO_3 and SO_4^- have similar reactivity toward X^- ions and the mechanism for $NO_3 + X^-$ reaction is an electron transfer process.

Atmospheric Implications. From the present and previously reported data, the reactive uptake coefficient, γ, of the NO_3 radical on water droplets with several dissolved ionic species can be calculated using the expression $\gamma^2 = \gamma_w^2 + (4RT/\omega)^2 \sum_i H^2 D_l k_i [X^-]$. For a cloud droplet with [Cl^-] = 1×10^{-4} M, [S(IV)] = 1×10^{-6} M, [HCOOH + $HCOO^-$] = 5×10^{-6} M, [$CH_3COOH + CH_3COO^-$] = 2×10^{-6} M, and pH = 5.0,[6,7,9] γ is estimated to be 2.2×10^{-4}. In this case, NO_3 is lost mostly

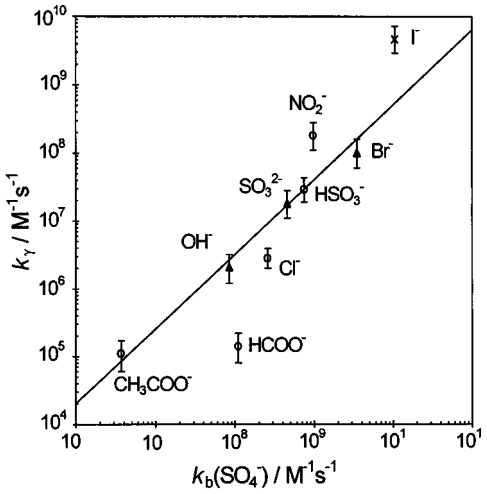

Figure 5. Comparison between rate coefficients of NO_3 reactions, k_γ's, obtained at 273 K in this work and those for corresponding SO_4^- reactions measured in the bulk at 298 K. Values of $k_b(SO_4^-)$ are obtained from Neta *et al.*[32] (solid triangles) and Wine *et al.*[33] (open circles). For reaction with I^-, calculated diffusion-controlled rate coefficient is used as $k_{9b}(SO_4^-)$ (cross). The error bars are 2σ and include precision and systematic errors. The solid line shows a linear correlation between $\log(k_\gamma)$ and $\log(k_b(SO_4^-))$ excluding the reactions with $HCOO^-$ and I^- ions.

via reaction with H_2O, reaction 1. If the concentration of [S(IV)] were an order of magnitude higher, reaction with HSO_3^- would be competing with reaction 1. The reactions with $HCOO^-$ (reaction 9) and CH_3COO^- (reaction 10) at the above concentrations would have negligible contribution to the NO_3 loss rate constant. For a cloud with 40 droplets cm^{-3} of 3×10^{-3} cm diameter droplets,[7] NO_3 lifetime due to heterogeneous loss will be ~500 s. This estimated lifetime is comparable to or shorter than that due to the loss via uptake of N_2O_5:

$$NO_3 + NO_2 + M \rightarrow N_2O_5 + M \qquad (14)$$

followed by

$$N_2O_5(g) + H_2O(l) \rightarrow 2\,HNO_3(aq) \qquad (15)$$

Therefore, reactive uptake of NO_3 onto clouds would have an impact on the concentration of NO_3 in the gas phase.

The reactive uptake of NO_3 is important not only for the NO_3 loss in the gas phase but also for the oxidation of species in the solution. For example, reactions 9 and 10, while they are a minor contributor to NO_3 loss, are sink processes for $HCOO^-$ and CH_3COO^- ions in droplets during the night. They generate HCOO and CH_3COO radicals which instantly decompose to give $H + CO_2$ and $CH_3 + CO_2$, respectively. Thus, they will destroy the acids and generate new radicals. The uptake of NO_3 can also initiate the catalytic oxidation of S(IV) to S(VI), both directly and indirectly, in clouds.[34]

Acknowledgment. The authors acknowledge the help of R. B. Norton for the ion chromatographic analysis of the liquid samples. This work was funded in part by NOAA's Climate and Global Change research program. This work was performed while T.I. and Y.R. held National Research Council−NOAA research fellowships.

Appendix

The average concentration of H^+, $[H^+]_s$, in the liquid surface (thickness $l = (D_l/k_l')^{1/2}$) formed due to the uptake of N_2O_5 was estimated using the plug flow approximation. To simplify our argument, we assume that gaseous N_2O_5 is introduced into the reactor through the injector at $z = 0$ and is taken up into water with $\gamma = 1$, which results in the conversion into $2(H^+ + NO_3^-)$.

It is assumed that N_2O_5 decays due to the uptake into water with a gas phase diffusion-limited rate coefficient k_{dl}, which is estimated to be 42 s^{-1} (P_{total} = 13.5 Torr) using the diffusion coefficients of 290 and 64 Torr cm^2 s^{-1} for N_2O_5 in He and in H_2O, respectively.[22,35] In the flow reactor, the gas−liquid contact time, t_c ($=L/v_l$, where v_l is the flow velocity of liquid film), below the injector (reaction length $L \sim 30$ cm) is ~3 s. The total number of N_2O_5 molecules taken up after introduction into the reactor through the injector, $T_{N_2O_5}{}^T$, is calculated by

$$N_{N_2O_5}{}^T = J_0\{1 - \exp(-k_{dl}L/v_g)\}t_c \qquad (AI)$$

where J_0 is the flux of N_2O_5 into the gas phase through the injector and v_g is the gas flow velocity. The average formation rate of $H^+ + NO_3^-$ was calculated to be $\sim 1 \times 10^{-8}$ mol s^{-1}. This means that, during the contact time, 3×10^{-8} mol of H^+ ions is formed, which must correspond to the amount of $2N_{N_2O_5}{}^T$. Using the typical values of k_{dl} (42 s^{-1}) and v_g (850 cm s^{-1}), J_0 is calculated to be 6.7×10^{-9} mol s^{-1}.

The number of N_2O_5 molecules taken up into water (surface area $= 2\pi r\,\delta z$) per unit time at $z = (Z' - \delta z) \sim Z'$ downstream the injector is given by

$$\Delta J_{N_2O_5}(Z') = J_0 \exp(-k_{dl}Z'/v_g)(k_{dl}/v_g)\,\delta z \qquad (AII)$$

Because of the rapid hydrolysis of N_2O_5, H^+ is immediately formed at the surface. The number of H^+ formed at the surface due to the uptake of N_2O_5 is given by

$$N_0(Z') = 2\Delta J_{N_2O_5}(Z')(\delta z/v_l) \qquad (AIII)$$

Protons formed at $z = Z'$ diffuse into the bulk while the liquid film flows down the reactor, and at $z = Z$ the concentration profile of H^+ formed at $z = Z'$, $C'(x,Z')$, is given as a function of the distance x from the surface:[26]

$$C'(x,Z') = \frac{N_0(Z')}{A\sqrt{\pi D_l t}} \exp\left(-\frac{x^2}{4D_l t}\right) \qquad (AIV)$$

where $t = (Z - Z')/v_l$ and $A = 2\pi r\,\delta z$. The concentration $C(x,Z)$ of H^+ at $z = Z$ is obtained by integrating the contribution of H^+ injected at $z = 0$ to Z,

$$C(x,Z) = \lim_{\delta z \to 0} \int_0^{Z-\delta z} C'(x,Z')\,dZ' \qquad (AV)$$

The average H^+ concentration in the liquid surface with the thickness of l at $z = Z$, $[H^+]_s{}^{av}(Z)$, is given by

$$[H^+]_s{}^{av}(Z) \le C(x{=}0,Z) \qquad (AVI)$$

In our calculation, δz was assumed to be $\le l \times 10^{-2}$ (for $l = 10^{-3}$−10^{-7} cm), which corresponds to a shorter mixing time than the reaction time of NO_3 in the liquid. Using the typical values, i.e., $J_0 = 6.7 \times 10^{-9}$ mol s^{-1}, $v_g = 850$ cm s^{-1}, $v_l = 10$ cm s^{-1}, and $D_l = 10^{-5}$ cm^2 s^{-1} for NO_3 and H^+, $[H^+]_s{}^{av}(Z)$ was obtained to be $\le 3 \times 10^{-5}$ M.

References and Notes

(1) Atkinson, R. *J. Phys. Chem. Ref. Data* **1991**, *20*, 459.
(2) Wayne, R. P.; Barnes, I.; Biggs, P.; Burrows, J. P.; Canosa-Mas, C. E.; Hjorth, J.; Le Bras, G.; Moortgat, G. K.; Perner, D.; Poulet, G.; Restelli, G.; Sidebottom, H. *Atmos. Environ.* **1991**, *25A*, 1.
(3) Chameides, W. L. *J. Geophys. Res.* **1986**, *91*, 5331.
(4) Chameides, W. L. *J. Geophys. Res.* **1986**, *91*, 14571.
(5) Mozurkewich, M. *J. Geophys. Res.* **1986**, *91*, 14569.

(6) Sander, R.; Lelieveld, J.; Crutzen, P. J. *J. Atmos. Chem.* **1995**, *20*, 89.
(7) Graedel, T. E.; Crutzen, P. J. *Atmospheric Change—An Earth System Perspective*; W. H. Freeman and Company: New York, 1993.
(8) Munger, J. W.; Jacob, D. J.; Waldman, J. M.; Hoffmann, M. R. *J. Geophys. Res.* **1983**, *88*, 5109.
(9) Keene, W. C.; Galloway, J. N. *J. Geophys. Res.* **1986**, *91*, 14466.
(10) Daniels, M. *J. Phys. Chem.* **1969**, *73*, 3710.
(11) Kim, K.-J.; Hamill, W. H. *J. Phys. Chem.* **1976**, *80*, 2320.
(12) Neta, P.; Huie, R. E. *J. Phys. Chem.* **1986**, *90*, 4644.
(13) Exner, M.; Herrmann, H.; Zellner, R. *Ber. Bunsen-Ges. Phys. Chem.* **1992**, *96*, 470.
(14) Exner, M.; Hermann, H.; Zellner, R. *J. Atmos. Chem.* **1994**, *18*, 359.
(15) Rudich, Y.; Talukdar, R. K.; Fox, R. W.; Ravishankara, A. R. *J. Geophys. Res.* **1996**, *101*, 21023.
(16) Rudich, Y.; Talukdar, R. K.; Imamura, T.; Fox, R. W.; Ravishankara, A. R. *Chem. Phys. Lett.* **1996**, *261*, 467.
(17) Vogel, A. I. *A Text-Book of Quantitative Inorganic Analysis*; John Wiley & Sons Inc.: New York, 1961.
(18) Brown, R. L. *J. Res. Natl. Bur. Stand. (U.S.)* **1978**, *83*, 1.
(19) Howard, C. J. *J. Phys. Chem.* **1979**, *83*, 3.
(20) Danckwerts, P. V. *Gas-Liquid Reactions*; McGraw-Hill: New York, 1970.
(21) Jayne, J. T.; Gardner, J. A.; Davidovits, P.; Worsnop, D. R.; Zahniser, M. S.; Kolb, C. E. *J. Geophys. Res.* **1990**, *95*, 20559.
(22) Hanson, D. R.; Burkholder, J. B.; Howard, C. J.; Ravishankara, A. R. *J. Phys. Chem.* **1992**, *96*, 4979.
(23) Kolb, C. E.; Worsnop, D. R.; Zahniser, M. S.; Davidovits, P.; Keyser, L. F.; Leu, M. T.; Molina, M. J.; Hanson, D. R.; Ravishankara, A. R.; Williams, L. R.; Tolbert, M. A. Laboratory Experiments of Atmospheric Heterogeneous Chemistry. In *Progress and Problems in Atmospheric Chemistry*; Barker, J. R., Ed.; Advances in Physical Chemistry Series; World Scientific Publishing Co.: Singapore, 1995; Vol. 3, p 771.
(24) Moore, W. J. *Basic Physical Chemistry*; Prentice-Hall, Inc.: Englewood Cliffs, NJ, 1983.
(25) *CRC Handbook of Chemistry and Physics*, 70th ed.; CRC Press: Cleveland, 1990.
(26) Atkins, P. W. *Physical Chemistry*, 4th ed.; Oxford University Press: New York, 1990.
(27) Wine, P. H.; Mauldin, R. L.; Thorn, R. P. *J. Phys. Chem.* **1988**, *92*, 1156.
(28) CRC. *Handbook of Chemistry and Physics*, 60th ed.; CRC Press: Cleveland, 1987.
(29) Marcus, R. J. *Rev. Mod. Phys.* **1993**, *65*, 599.
(30) Logager, T.; Sehested, K.; Holcman, J. *Radiat. Phys. Chem.* **1993**, *41*, 539.
(31) Huie, R. E. Free Radical Chemistry of the Atmospheric Aqueous Phase. In *Progress and Problems in Atmospheric Chemistry*; Barker, J. R., Ed.; Advances in Physical Chemistry Series; World Scientific Publishing Co.: Singapore, 1995; Vol. 3, p 374.
(32) Neta, P.; Huie, R. E.; Ross, A. B. *J. Phys. Chem. Ref. Data* **1988**, *17*, 1027.
(33) Wine, P. H.; Tang, Y.; Thorn, R. P.; Wells, J. R. *J. Geophys. Res.* **1989**, *94*, 1085.
(34) Rudich, Y.; Talukdar, R. K.; Ravishankara, A. R. *Geophys. Res. Lett.* In preparation.
(35) Hanson, D. R.; Ravishankara, A. R. *J. Geophys. Res.* **1991**, *96*, 5081.
(36) Stanbury, D. M. *Adv. Inorg. Chem.* **1989**, *33*, 69.